

Electronic Supplementary Information to:

Optically Active Covalent Organic Frameworks and Hyperbranched Polymers with Chirality Induced by Circularly Polarized Light

Yuting Wang,^a Koji Yazawa,^b Qingyu Wang,^a Takunori Harada,^c Shuhei Shimoda,^d Zhiyi Song,^a Masayoshi Bando,^a Naofumi Naga,^e and Tamaki Nakano^{*a,f}

^aInstitute for Catalysis (ICAT) and Graduate School of Chemical Sciences and Engineering
Hokkaido University, N21W10, Kita-ku, Sapporo 001-0021, Japan

E-mail: tamaki.nakano@cat.hokudai.ac.jp

^bJEOL RESONANCE Inc., 3-1-2 Musashino, Akishima, Tokyo 196-8558, JAPAN

^cDepartment of Integrated Science and Technology, Faculty of Science and Technology
Oita University, Dannoharu, 700, Oita City 870-1192, Japan

^dTechnical Division, Institute for Catalysis (ICAT), Hokkaido University, N21W10, Kita-ku,
Sapporo 001-0021, Japan

^eDepartment of Applied Chemistry, Shibaura Institute of Technology, College of Engineering,
3-7-5 Toyosu, Koto-ku, Tokyo 135-8548, Japan

^fIntegrated Research Consortium on Chemical Sciences (IRCCS), Institute for Catalysis,
Hokkaido University, N21W10, Kita-ku, Sapporo 001-0021, Japan

*Correspondence should be addressed to Tamaki Nakano (E-mail:
tamaki.nakano@cat.hokudai.ac.jp)

Table of Contents

Experimental details	2
Conditions and results of polymerization (Tables)	6
¹³ C NMR spectra of soluble HBP's	8
CMPAS ¹³ C NMR spectra and related data of insoluble COF's	10
IR spectra	15
DSC and TGA profiles	17
DLS profiles	18
TEM and XRD profiles	19
gCD-UV spectra	21
LD spectra	31
N ₂ gas absorption (BET analysis)	33
References	34

Experimental

Materials. Benzene-1,4-diboronic acid (TCI), (1,1'-biphenyl)-4,4'-diyl diboronic acid (TCI), 4,4''-dibromo-1,1':4',1''-terphenyl (TCI), 1,3,5-tribromobenzene (TCI), bis(pinacolato)diboron (Kanto Chemical), tetrakis(triphenylphosphine)palladium(0) (TCI), palladium(II) dichloride (Aldrich), triphenylphosphine (Kanto Chemical), 1,2-dimethoxyethane (TCI), dioxane (TCI) and 4-methyltetrahydropyran (TCI) were used as purchased.

General instrumentation. ¹H NMR spectra in solution were recorded on a JEOL JNM-ECX400 spectrometer (400 MHz for ¹H measurement) and a JEOL JNM-ECA600 spectrometer (600 MHz for ¹H measurement). SEC measurements were carried out using a chromatographic system consisting of a Hitachi L-7100 chromatographic pump, a Hitachi L-7420 UV detector (254 nm), and a Hitachi L-7490 RI detector equipped with series (eluent THF, flow rate 1.0 mL/min). UV-vis absorption spectra were measured at room temperature with a JASCO V-570 spectrophotometers. Steady-state emission spectra were taken on a JASCO FP-8500 fluorescence spectrophotometer. IR spectra were recorded on a JASCO FT/IR-6100 spectrometer using KBr pellet samples. Circular dichroism (CD) and linear dichroism (LD) spectra were taken with a JASCO-820 spectrometer. The spectra were obtained by averaging those recorded at four (90° interval) different film orientations (angles) with the film face positioned vertically to the incident light beam for measurement. LD contributions were thus minimized to afford true CD spectra. The anisotropy factor (g_{CD}) was calculated according to $g_{CD} = \Delta Abs / Abs = (\text{ellipticity} / 32980) / Abs$. Differential scanning calorimetry (DSC) and thermal gravity analysis (TGA) were taken on Rigaku Thermo Plus DSC8230 and TG8120 analyzer at a heating rate of 10 K/min in nitrogen atmosphere. Surface area and pore volume were measured by nitrogen sorption using an Autosorb 6AG apparatus (Quantachrome, FL, USA) based on the Brunauer-Emmett-Teller (BET) equation. Transmission electron microscopy images were acquired with a JEM-2100F microscope at an accelerating voltage of 200 kV. Scanning electron microscope images were acquired with a JSM-7400F microscope at an accelerating voltage of 3 kV. Dynamic light scattering (DLS) experiment was conducted using a NICOMP 380 ZLS Particle Sizer. Wide-angle X-ray diffraction (XRD) patterns were measured using Rigaku MiniFlex600-C ($\lambda = 1.54 \text{ \AA}$ (Cu K α)).

Solid-state NMR. The solid-state NMR experiments were performed at 600.17 MHz for ¹H and at ¹³C 150.91 MHz for ¹³C using a JEOL JNM-ECZR system equipped with a JEOL 3.2 mm extended VT probe. Experimental ¹³C shifts were referenced to TMS at 0 ppm with sample substitution referencing to the adamantane methylene at 37.77 ppm.¹ $\pi/2$ pulse lengths

of 2.3 and 2.2 μs were applied for ^{13}C and ^1H , respectively. The ^{13}C Cross Polarization with Magic Angle Spinning (CPMAS) spectra were acquired under MAS at 20kHz, using 2ms of ramped-amplitude CP, TPPM ^1H decoupling² with a decoupling field of 109kHz and 2s of recycle delay. The ^{13}C longitudinal relaxation times in a rotating frame ($T_{1\rho}^{\text{C}}$) were obtained by the CPMAS with spin lock method under 10kHz MAS. The spin lock lengths were varied from 0.1ms to 50ms under 54kHz of spin lock field.

The Center band Only Detection of Exchange (CODEX) measurements³ were performed under 10kHz MAS using mixing times, t_m , ranging from 1 to 500ms with a 0.2ms of chemical shift anisotropy recoupling time, Nt_r . The CODEX intensity S is subtracted from that of the reference spectrum S_0 , which contains the same relaxation factors but without motion effects during t_m , to obtain the pure-exchange intensity, $\Delta S = S - S_0$, which contains only contributions of the slow mobile segments. The correlation time τ_c was determined from t_m -dependence of the normalized CODEX intensities, $\Delta S/S_0$, with the equation $\Delta S/S_0 = 1 - \exp(-\tau_c/t_m)^\beta$, where β is stretched exponential coefficient.

The sample temperature was calibrated using $\text{Pb}(\text{NO}_3)_2$ as an NMR thermometer.

1,3,5-tris(4,4,5,5-tetramethyl-1,3,2-dioxaborolan-2-yl)benzene.⁴

1,3,5-Tribromobenzene (7.87 g, 25.0 mmol), bis(pinacolato)diboron (20.95 g, 82.5 mmol), KOAc (8.10 g, 82.5 mmol) and bis(triphenylphosphine)palladium(II) dichloride (1.75 g, 2.50 mmol) were mixed with degassed dioxane (200 mL) in a 500-mL flask, and the reaction mixture was stirred at 120°C for 24 h. After the mixture was cooled at r.t., raw products were collected by filtration, dried under reduced pressure, and recrystallized from EtOAc to lead to a white powder as the pure monomer: yield 6.93 g, (61 %). ^1H NMR (400 MHz, CDCl_3 , r.t.): 8.36 ppm (3H, s), 1.33 ppm (36H, s). FT-IR (KBr) ν/cm^{-1} : 2980, 2931, 1594, 1342, 1328, 1270, 1214, 1144, 1006, 968, 912, 886, 849, 721, 692, 642, 579.

Poly(benzene-1,3,5-triyl-*alt*-benzene-1,4-diyl). A typical procedure of synthesis and purification follows (run 4 in Table S1). To a 1,3,5-tribromobenzene (0.1 mol, 31.5 mg) in a degassed 1,2-dimethoxyethane (2 mL) solution was added benzene-1,4-diboronic acid (0.3 mmol, 49.7 mg) in a degassed aqueous solution of K_2CO_3 (2 M, 0.325 mL). $\text{Pd}(\text{PPh}_3)_4$ (10 mol%) was then introduced, and the reaction mixture was stirred under N_2 at 80°C for 24 h. The reaction mixture was quenched by the addition of aq. HCl solution (2 N, 0.65 mL). Crude products were washed with H_2O (40 mL \times 2 times) and methanol (40 mL \times 3 times) in this order and collected with a centrifuge. The washed material was reprecipitated in tetrahydrofuran (THF) (40 mL) and collected with a centrifuge, which was repeated three times, resulting in THF-insoluble COF and THF-soluble HBP samples.

THF-soluble HBP: ^1H NMR (400 MHz, CDCl_3 , r.t.): 8.0-6.9 ppm (aromatic area). ^{13}C NMR (100 MHz, CDCl_3 , r.t.): 136-135, 131-124 ppm (aromatic area); FT- IR (KBr) ν/cm^{-1} : 3033, 1724, 1596, 1511, 1437, 1386, 1234, 1176, 1118, 1074, 1036, 968, 922, 883, 825, 791, 765, 724, 697, 540.

THF-insoluble COF: FT- IR (KBr) ν/cm^{-1} : 3029, 1772, 1594, 1514, 1478, 1437, 1383, 1265, 1227, 1173, 1118, 1103, 1033, 1016, 886, 825, 791, 765, 743, 724, 697, 567, 540. Anal. Calcd for $(\text{C}_{30}\text{H}_{18})_n$: C, 95.24; H, 4.76. Found: C, 79.31; H, 4.87; Br, 3.23.

Poly(benzene-1,3,5-triyl-*alt*-1,1'-biphenyl-4,4''-diyl). A typical procedure of synthesis and purification follows (run 3 in Table S1). To a 1,3,5-tribromobenzene (0.1 mol, 31.48 mg) in a degassed 1,2-dimethoxyethane solution (2 mL) was added 1,1'-biphenyl-4,4''-diyl diboronic acid (0.2 mmol, 48.4 mg) in a degassed aqueous solution of K_2CO_3 (2 M, 0.325 mL). $\text{Pd}(\text{PPh}_3)_4$ (10 mol%) was then introduced, and the reaction mixture was stirred under N_2 at 80°C for 24 h. The reaction mixture was quenched by the addition of aq. HCl solution (2 N, 0.65 mL). Crude products were washed with H_2O (40 mL \times 2 times) and methanol (40 mL \times 3 times) in this order and collected with a centrifuge. The washed material was reprecipitated in tetrahydrofuran (THF) (40 mL) and collected with a centrifuge, which was repeated three times, resulting in THF-insoluble COF and THF-soluble HBP samples.

THF-soluble HBP: ^1H NMR (400 MHz, CDCl_3 , r.t.): 8.0-6.9 ppm (aromatic area). ^{13}C NMR (100 MHz, CDCl_3 , r.t.): 136-134, 132-126 ppm (aromatic area); FT-IR (KBr) ν/cm^{-1} : 3029, 1608, 1591, 1523, 1499, 1437, 1389, 1364, 1260, 1224, 1190, 1171, 1112, 1067, 1038, 1004, 958, 922, 816, 765, 741, 726, 698, 639, 613, 579, 518.

THF-insoluble COF: FT-IR (KBr) ν/cm^{-1} : 3029, 1591, 1499, 1434, 1388, 1340, 1260, 1171, 1118, 1038, 1002, 813, 765, 748, 726, 694. Anal. Calcd for $(\text{C}_{48}\text{H}_{30})_n$: C, 95.05; H, 4.95. Found: C, 83.74; H, 4.92; Br, 1.05.

Poly(benzene-1,3,5-triyl-*alt*-1,1':4',1''-terphenyl-4,4''-diyl). A typical procedure of synthesis and purification follows (run 3 in Table S3-2). To a 1,3,5-tris(4,4,5,5-tetramethyl-1,3,2-dioxaborolan-2-yl)benzene (1 mmol, 456 mg) in a degassed 1,2-dimethoxyethane (20 mL) solution was added 4,4''-dibromo-1,1':4',1''-terphenyl (2 mmol, 776.2 mg) in a degassed aqueous solution of K_2CO_3 (2 M, 3.25 mL). $\text{Pd}(\text{PPh}_3)_4$ (10 mol%) was then introduced, and the reaction mixture was stirred under N_2 at 80°C for 24 h. The reaction mixture was quenched by the addition of aq. HCl solution (6.5 mL). The crude product was washed by Crude products were washed with H_2O (40 mL \times 2 times) and methanol (40 mL \times 3 times) in this order and collected with a centrifuge. The washed material was reprecipitated in tetrahydrofuran

(THF) (40 mL) and collected with a centrifuge, which was repeated three times, resulting in THF-insoluble COF and THF-soluble HBP samples. THF-insoluble COF was further purified by Soxhlet extraction with CHCl₃ for 12 h.

THF-soluble HBP: ¹H NMR (400 MHz, CDCl₃, r.t.): 8.5-6.9 ppm (aromatic area). ¹³C NMR (100 MHz, CDCl₃, r.t.): 133-131, 129-127 ppm (aromatic area); FT- IR (KBr) ν/cm^{-1} : 3033, 2974, 1592, 1437, 1379, 1321, 1263, 1141, 1115, 999, 806, 696, 542.

THF-insoluble COF: FT- IR (KBr) ν/cm^{-1} : 3024, 1593, 1484, 1437, 1389, 1173, 1110, 1106, 807, 743, 695, 536. Anal. Calcd for (C₆₆H₄₂)_n: C, 94.96; H, 5.04. Found: C, 77.07; H, 4.72; Br, 9.12.

Film fabrication and CPL irradiation. HBP films were prepared from a chloroform solution by drop-casting on to a quartz plate (1 cm x 2 cm x 0.1 cm). The film thickness was around 1 μm as measured using a Keyence VK-X3000 (interference laser microscope).

CPL was generated by passing light from an Ushio Optical Modulex SX-UID500MAMQQ 500-W Hg-Xe lamp through a Gran-Taylor prism and a Fresnel Rhomb (50 mW (Jsec⁻¹)).

Calculation of relative irradiation energy sum (or relative absorbed dose). Because absorbance spectra changed as well as CD spectra on CPL irradiation, changes in g_{CD} value cannot be quantitatively discussed against simple irradiation time but should be discussed against terms of the “relative irradiation energy sum” which corresponds to the sum of irradiation time intervals (Δt_i) used to change a CD spectrum to the directly following CD spectrum multiplied by UV absorbance (Abs_i) corresponding to the former CD spectrum according to the following equation:

$$\text{Relative irradiation energy sum} = \sum_{i=0}^n \Delta t_i \times \text{Abs}_i$$

where absorbance intensity was measured at wavelengths designated in Figs. 1 and 2 in the main document.

Table S1. Synthesis of Poly(Bz135-*alt*-Bz14) COF and HBP in 1,2-dimethoxyethane at 80°C using Pd(PPh₃)₄ for 24 h^a

Run	[L]/[C] in feed	Conv. ^b (%)	MeOH-insoluble product			
			THF-insol. (COF)	THF-sol. (HBP)		
			Yield (%)	Yield (%)	M_n^c	M_w/M_n^c
1	1/1	90	0	47	430	1.50
2	1.5/1	>99	0	45	240	2.04
3	2/1	>99	51	21	580	1.88
4	3/1	>99	44	41	980	1.76
5	4/1	>99	92	15	860	1.47

^aC = 0.1 mmol, [C] = 0.05 M, [Pd(PPh₃)₄] = 0.005 M (10 mol% with respect to C).

^bDetermined by ¹H NMR analysis of reaction mixture (conversion of C).

^cDetermined by SEC using polystyrene standard.

Table S2. Synthesis of Poly(Bz135-*alt*-BP44') COF and HBP in 1,2-dimethoxyethane at 80°C using Pd(PPh₃)₄ for 24 h^a

Run	[L]/[C] in feed	Conv. ^b (%)	MeOH-insoluble product			
			THF-insol. (COF)	THF-sol. (HBP)		
			Yield (%)	Yield (%)	M_n^c	M_w/M_n^c
1	1/1	91	0	98	460	1.72
2	1.5/1	>99	4	97	520	1.86
3	2/1	>99	>99	<1	710	1.66
4	3/1	>99	79	18	920	1.60
5	4/1	>99	>99	<1	740	1.45

^aC = 0.1 mmol, [C] = 0.05 M, [Pd(PPh₃)₄] = 0.005 M (10 mol% with respect to C).

^bDetermined by ¹H NMR analysis of reaction mixture (conversion of C)

^cDetermined by SEC using polystyrene standard.

Table S3-1. Synthesis of Poly(Bz135-*alt*-TP44'') COF and HBP in 4-methyltetrahydropyran at 80°C using Pd(PPh₃)₄ for 24 h^a

Run	[L]/[C] in feed	Conv. ^b (%)	MeOH-insoluble product			
			THF-insol. (COF) Yield (%)	THF-sol. (HBP)		
				Yield ^c (%)	<i>M_n</i> ^d	<i>M_w</i> / <i>M_n</i> ^d
1	1/1	65	93	7	642	2.62
2	1.5/1	78	71	29	870	2.32
3	2/1	83	61	39	766	1.87
4	3/1	84	42	58	701	1.68
5	4/1	86	51	49	719	1.94

^aC = 0.5 mmol, [C] = 0.05 M, [Pd(PPh₃)₄] = 0.005 M (10 mol% with respect to C).

^bDetermined by ¹H NMR analysis of reaction mixture (conversion of C).

^cDetermined from conversion and yield of THF-insoluble POF.

^dDetermined by SEC using polystyrene standard.

Table S3-2. Synthesis of Poly(Bz135-*alt*-TP44'') COF and HBP in 1,2-dimethoxyethane at 80°C using Pd(PPh₃)₄ for 24 h^a

Run	[L]/[C] in feed	Conv. ^b (%)	MeOH-insoluble product			
			THF-insol. (COF) Yield (%)	THF-sol. (HBP)		
				Yield ^c (%)	<i>M_n</i> ^d	<i>M_w</i> / <i>M_n</i> ^d
1	1/1	>99	32	68	580	3.71
2	1.5/1	>99	12	88	720	1.88
3	2/1	85	12	73	660	2.32
4	3/1	>99	17	83	660	2.22
5	4/1	>99	45	55	700	2.66

^aC = 0.1 mmol (runs 1,2,4,5) 1 mmol (run 3), [C] = 0.05 M, [Pd(PPh₃)₄] = 0.005 M (10 mol% with respect to C).

^bDetermined by ¹H NMR analysis of reaction mixture (conversion of C).

^cDetermined from conversion and yield of THF-insoluble POF.

^dDetermined by SEC using polystyrene standard.

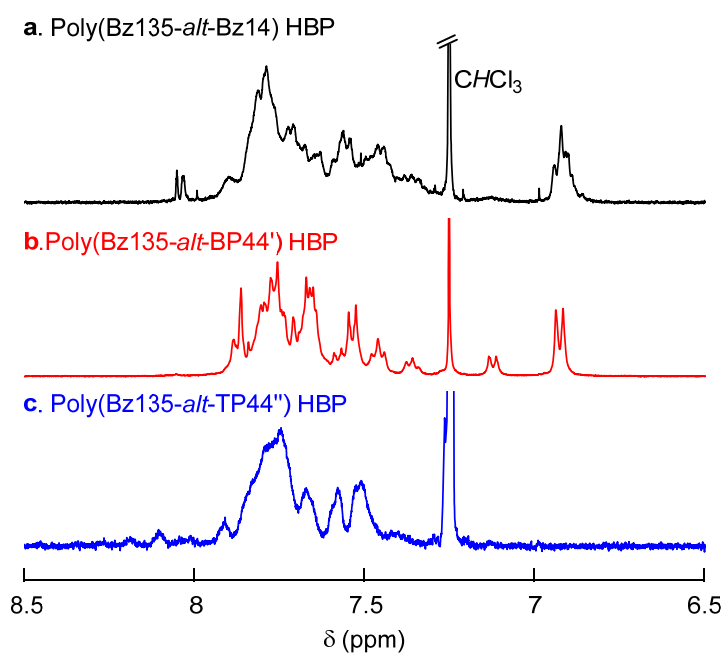


Fig. S1. ¹H NMR spectra of THF-soluble poly(Bz135-*alt*-Bz14) HBP (run 4 in Table S1) (a), poly(Bz135-*alt*-BP44') HBP (run 3 in Table S2) (b), and poly(Bz135-*alt*-TP44'') HBP (run 3 in Table S3-2) (c) [400 MHz, CDCl_3 , r.t.].

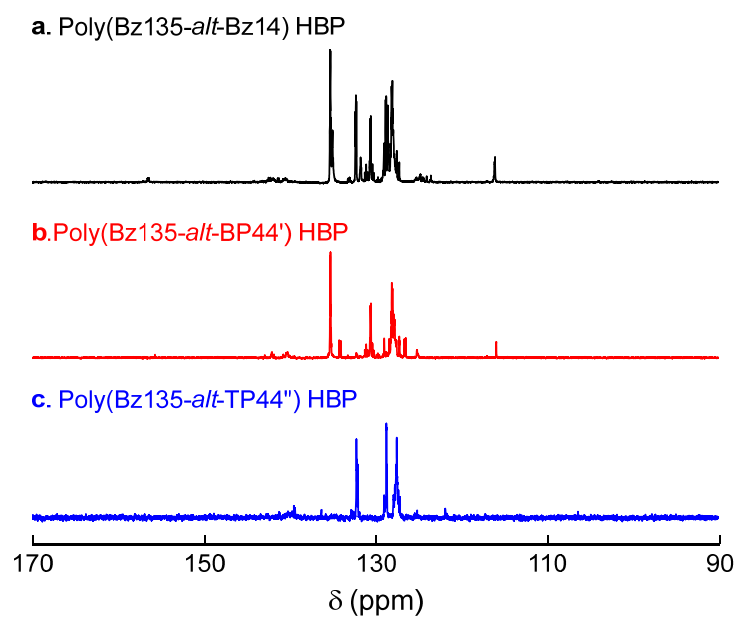


Fig. S2. ¹³C NMR spectra of THF-soluble poly(Bz135-*alt*-Bz14) HBP (run 4 in Table S1) (a), poly(Bz135-*alt*-BP44') HBP (run 3 in Table S2) (b), and poly(Bz135-*alt*-TP44'') HBP (run 3 in Table S3-2) (c) [150 MHz, CDCl₃, r.t.].

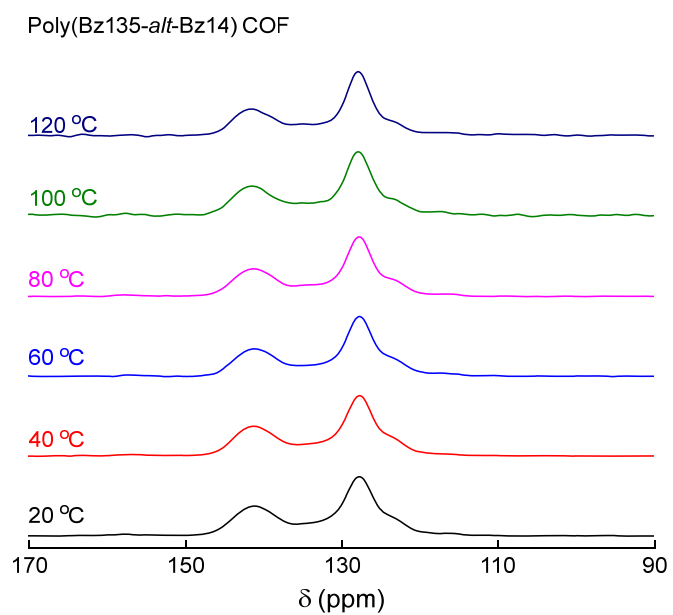


Fig. S3. ^{13}C CPMAS NMR spectra of THF-insoluble poly(Bz135-*alt*-Bz14) COF (run 4 in Table S1) observed at various temperatures.

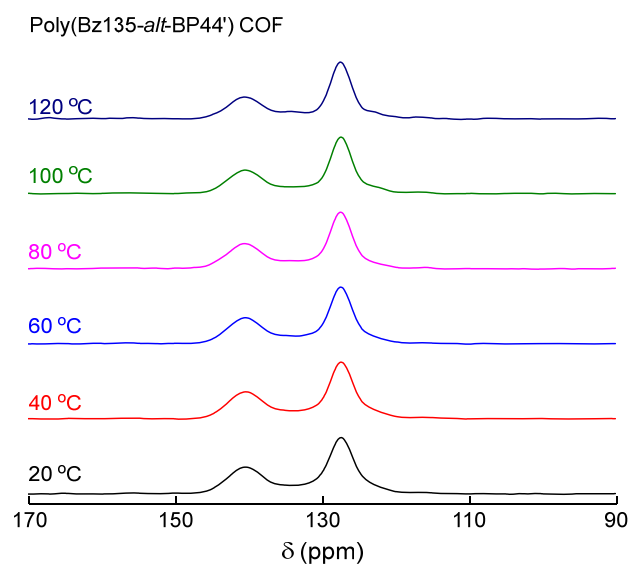


Fig. S4. ^{13}C CPMAS NMR spectra of THF-insoluble poly(Bz135-*alt*-BP44') COF (run 3 in Table S1) observed at various temperatures.

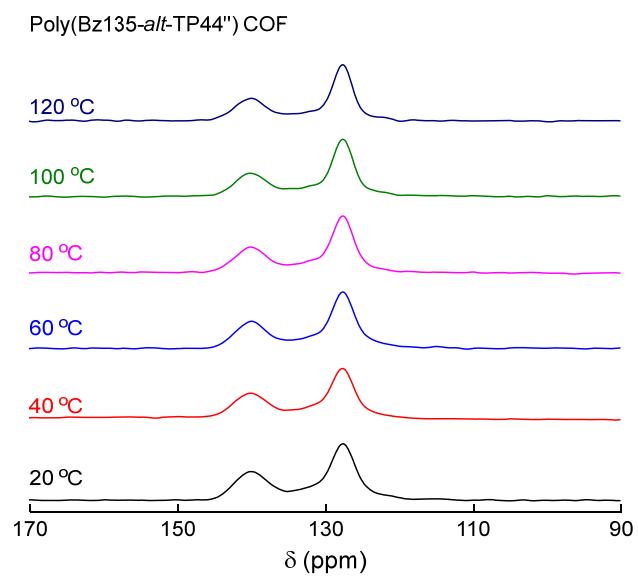


Fig. S5. ^{13}C CPMAS NMR spectra of THF-insoluble poly(Bz135-*alt*-TP44'') COF (run 3 in Table S3-2) observed at various temperatures.

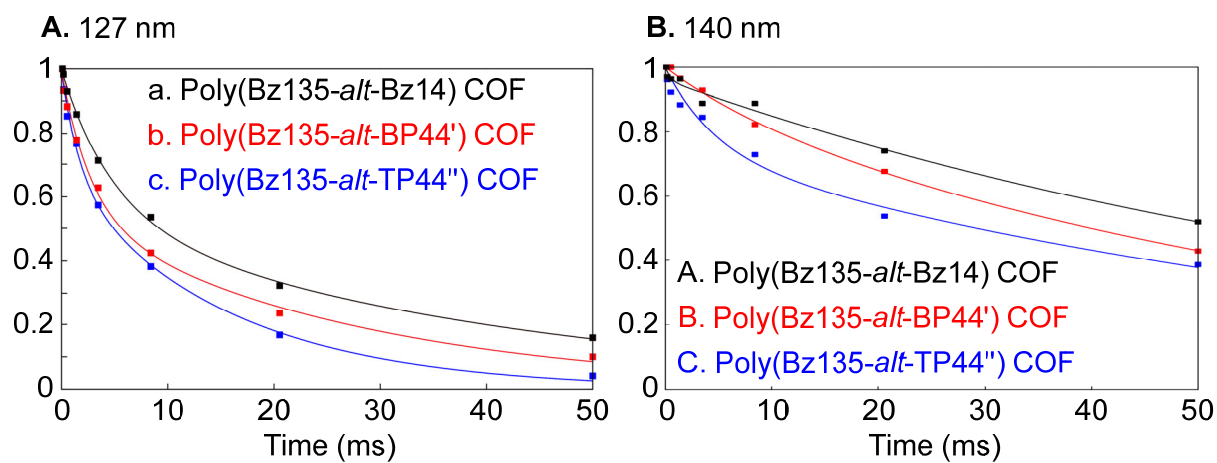


Fig. S6. Relaxation decay plots of ^{13}C $T_{1\rho}$ measurements for the signals at 127 ppm (A) and 140 ppm (B) of THF-insoluble poly(Bz135-*alt*-Bz14) COF (a) (run 4 in Table S1), poly(Bz135-*alt*-BP44') COF (b) (run 3 in Table S2), and poly(Bz135-*alt*-TP44'') COF (c) (run 3 in Table S3-1).

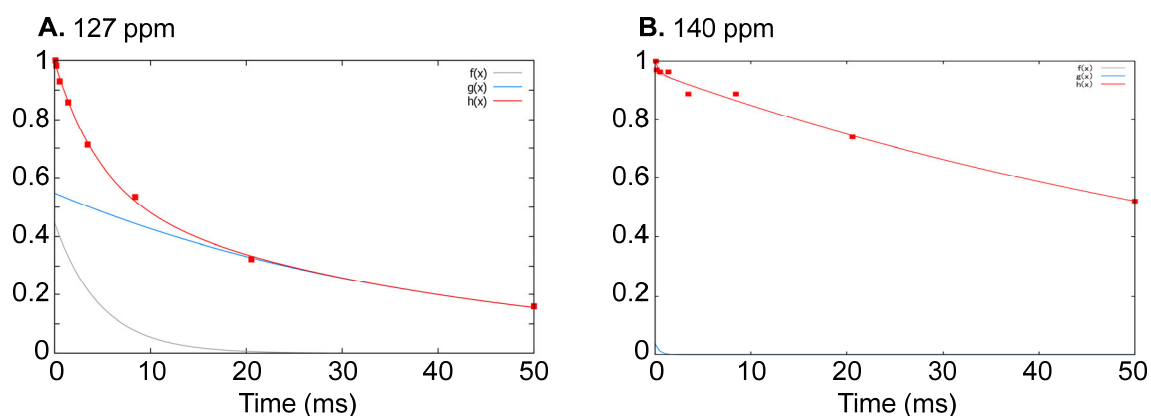


Fig. S7. Relaxation decay plots of ^{13}C $T_{1\rho}$ measurements for the signals at 127 ppm (A) and 140 ppm (B) of THF-insoluble poly(Bz135-*alt*-Bz14) COF (run 4 in Table S1) with exponential curve fitting.

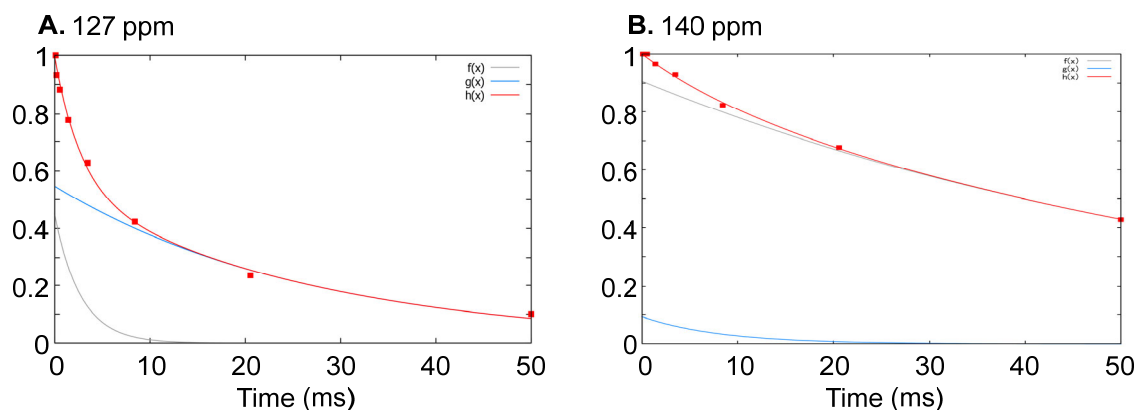


Fig. S8. Relaxation decay plots of ^{13}C $T_{1\rho}$ measurements for the signals at 127 ppm (A) and 140 ppm (B) of THF-insoluble poly(Bz135-*alt*-BP44') COF (run 3 in Table S2) with exponential curve fitting.

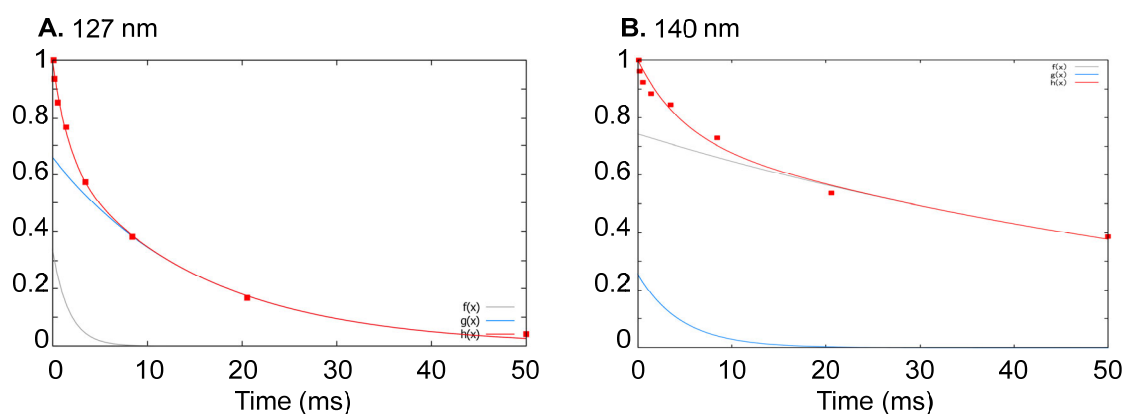


Fig. S9. Relaxation decay plots of ^{13}C $T_{1\rho}$ measurements at 127 ppm (A) and 140 ppm (B) of THF-insoluble poly(Bz135-*alt*-TP44'') COF (run 3 in Table S3-2) with exponential curve fitting.

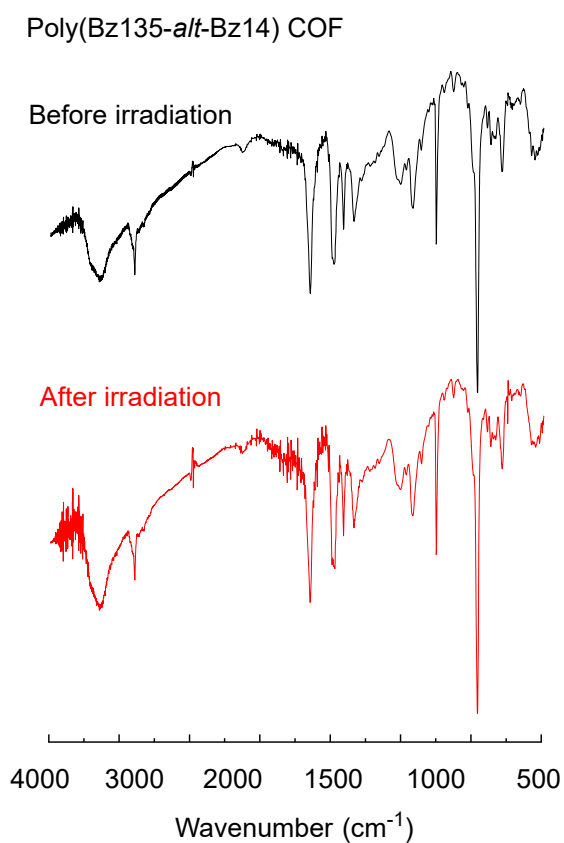


Fig. S10. IR spectra of THF-insoluble poly(Bz135-*alt*-TP44'') COF (run 3 in Table S3-2) before and after CPL irradiation. (Irradiation conditions: 500-W Hg-Xe lamp, L-CPL, 45 min).

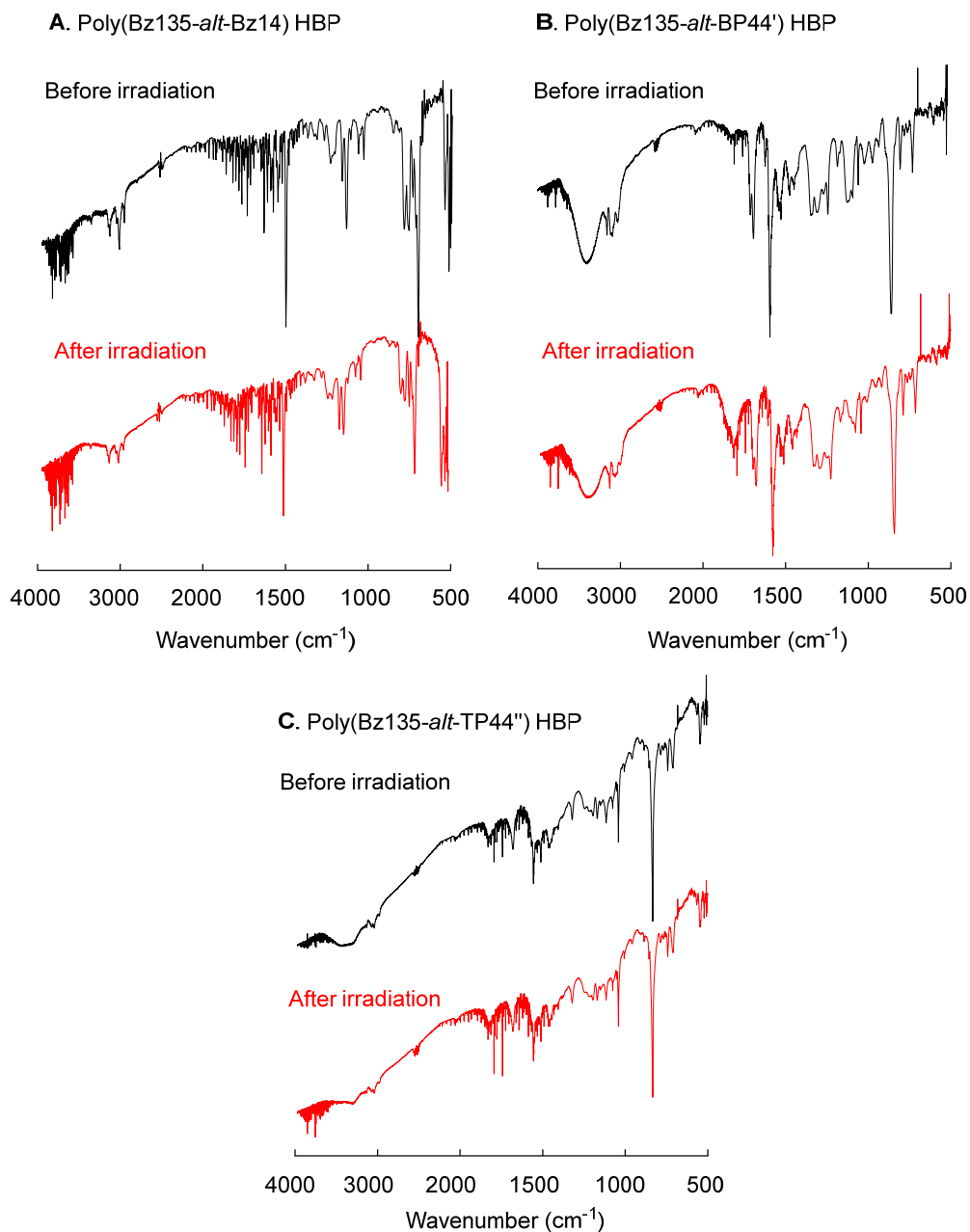


Fig. S11. IR spectra of THF-soluble poly(Bz135-*alt*-Bz14) HBP (A) (run 4 in Table S1), poly(Bz135-*alt*-BP44') HBP (B) (run 3 in Table S2), and poly(Bz135-*alt*-TP44'') HBP (C) (run 3 in Table S3) before and after CPL irradiation. (Irradiation conditions: 500-W Hg-Xe lamp, L-CPL, 20 min). [NaCl plate]

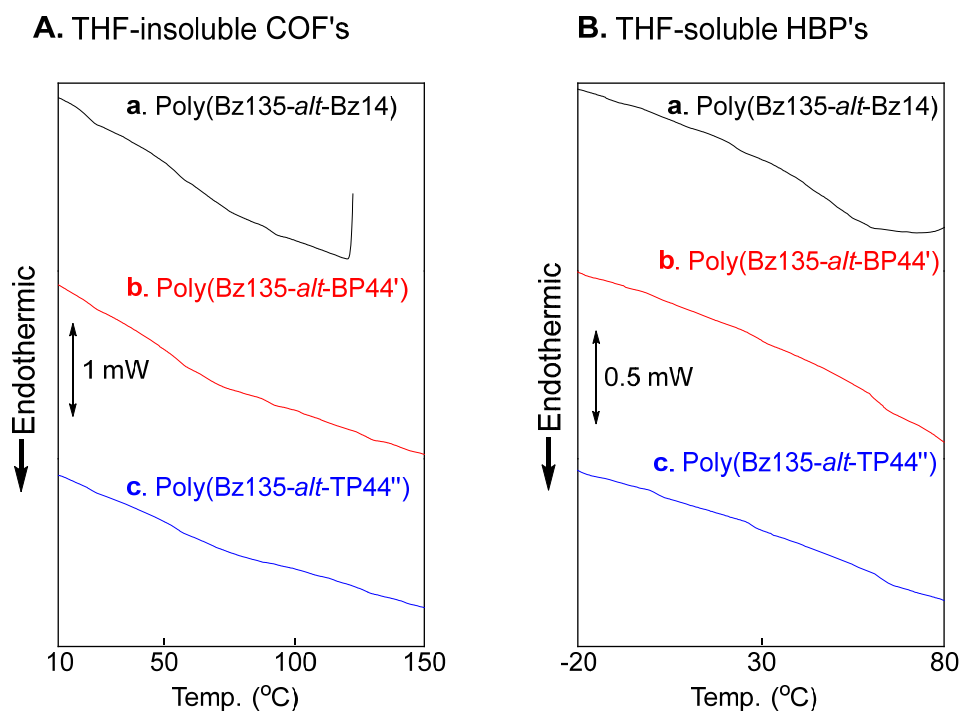


Fig. S12. DSC profiles of THF-insoluble COF's (A) and THF-soluble (B) HBP's: poly(Bz135-*alt*-Bz14) COF and HBP (run 4 in Table S1) (a), poly(Bz135-*alt*-BP44') COF and HBP (run 3 in Table S2) (b), and poly(Bz135-*alt*-TP44'') COF and HBP (run 3 in Table S3-1) (c).

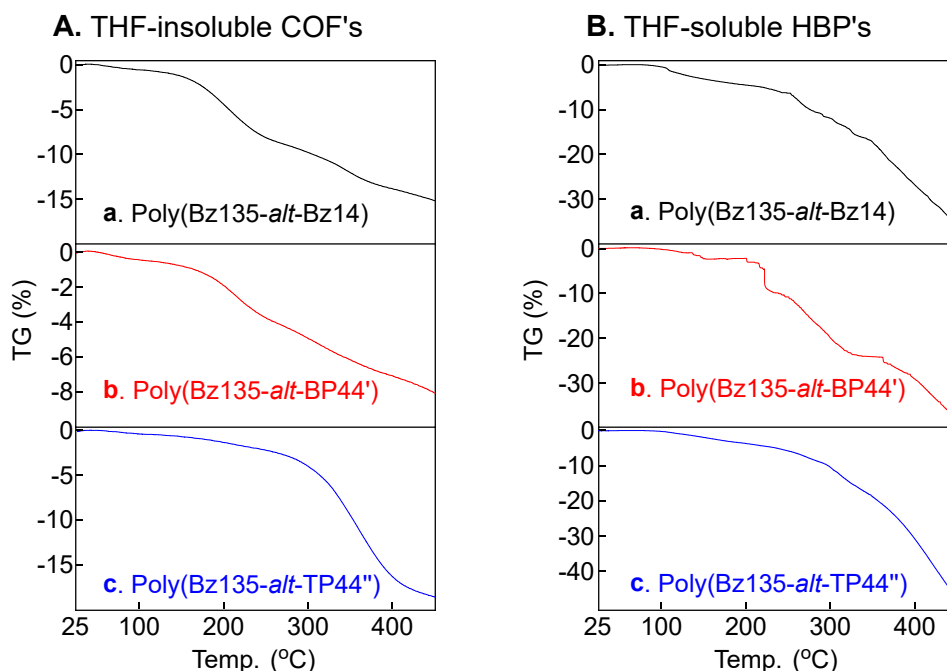
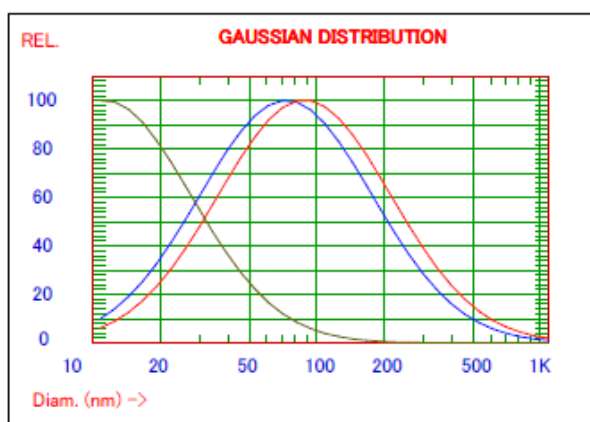


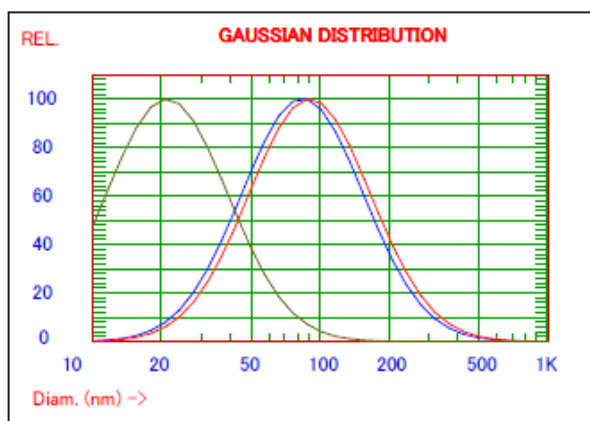
Fig. S13. TGA profiles of THF-insoluble COF's (A) and THF-soluble (B) HBP's: poly(Bz135-*alt*-Bz14) COF and HBP (run 4 in Table S1) (a), poly(Bz135-*alt*-BP44') COF and HBP (run 3 in Table S2) (b), and poly(Bz135-*alt*-TP44'') COF and HBP (run 3 in Table S3-1) (c).

A. Poly(Bz135-*alt*-Bz14) HBP



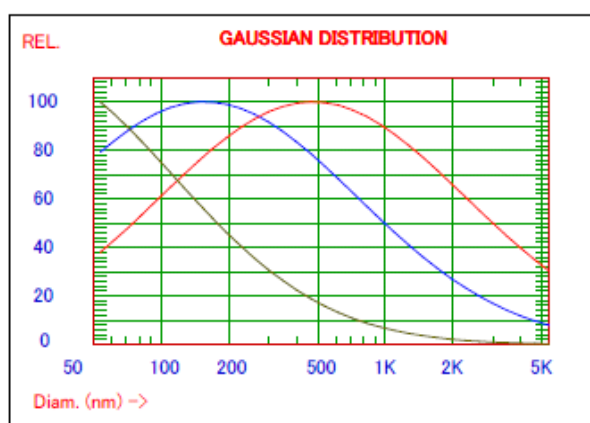
<i>Intensity Weighting:</i>	
Mean Diameter	= 108.5 nm
Std Deviation	= 96.6 nm (89.0 %)
<i>Volume Weighting:</i>	
Mean Diameter	= 131.2 nm
Std Deviation	= 116.8 nm (89.0 %)
<i>Number Weighting:</i>	
Mean Diameter	= 16.8 nm
Std Deviation	= 15.0 nm (89.0 %)

B. Poly(Bz135-*alt*-BP44') HBP



<i>Intensity Weighting:</i>	
Mean Diameter	= 101.2 nm
Std Deviation	= 62.5 nm (61.7 %)
<i>Volume Weighting:</i>	
Mean Diameter	= 109.0 nm
Std Deviation	= 67.3 nm (61.7 %)
<i>Number Weighting:</i>	
Mean Diameter	= 25.7 nm
Std Deviation	= 15.8 nm (61.7 %)

C. Poly(Bz135-*alt*-TP44'') HBP



<i>Intensity Weighting:</i>	
Mean Diameter	= 535.0 nm
Std Deviation	= 839.4 nm (156.9 %)
<i>Volume Weighting:</i>	
Mean Diameter	= 1624.1 nm
Std Deviation	= 2548.3 nm (156.9 %)
<i>Number Weighting:</i>	
Mean Diameter	= 81.0 nm
Std Deviation	= 127.0 nm (156.9 %)

Fig. S14. DLS profiles of THF-soluble poly(Bz135-*alt*-Bz14) HBP (run 4 in Table S1) (A), poly(Bz135-*alt*-BP44') HBP (run 3 in Table S2) (B), and poly(Bz135-*alt*-TP44'') HBP (run 3 in Table S3-2) (C) in THF. [conc. 1~3 M]

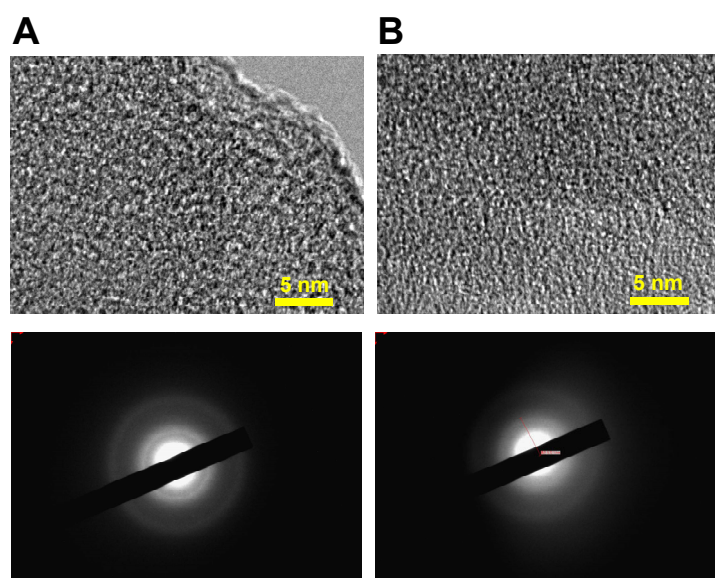


Fig. S15. TEM images (top) and electron diffraction profiles (bottom) of poly(Bz135-*alt*-BP44') COF (run 3 in Table S2 in the ESI) (A), and poly(Bz135-*alt*-TP44'') COF (run 3 in Table S3-2 in the ESI) (B).

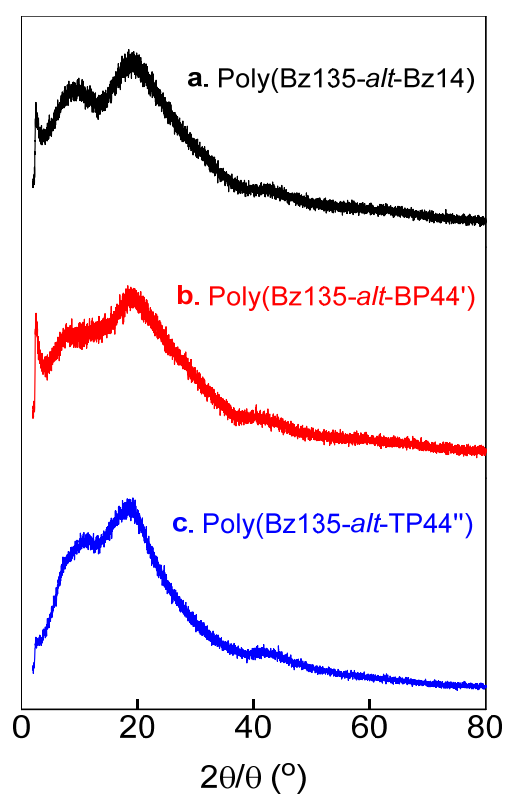


Fig. S16. XRD profiles of THF-insoluble poly(Bz135-*alt*-Bz14) COF (run 4 in Table S1) (a), poly(Bz135-*alt*-BP44') COF (run 3 in Table S2) (b), and poly(Bz135-*alt*-TP44'') COF (run 3 in Table S3-2) (c).

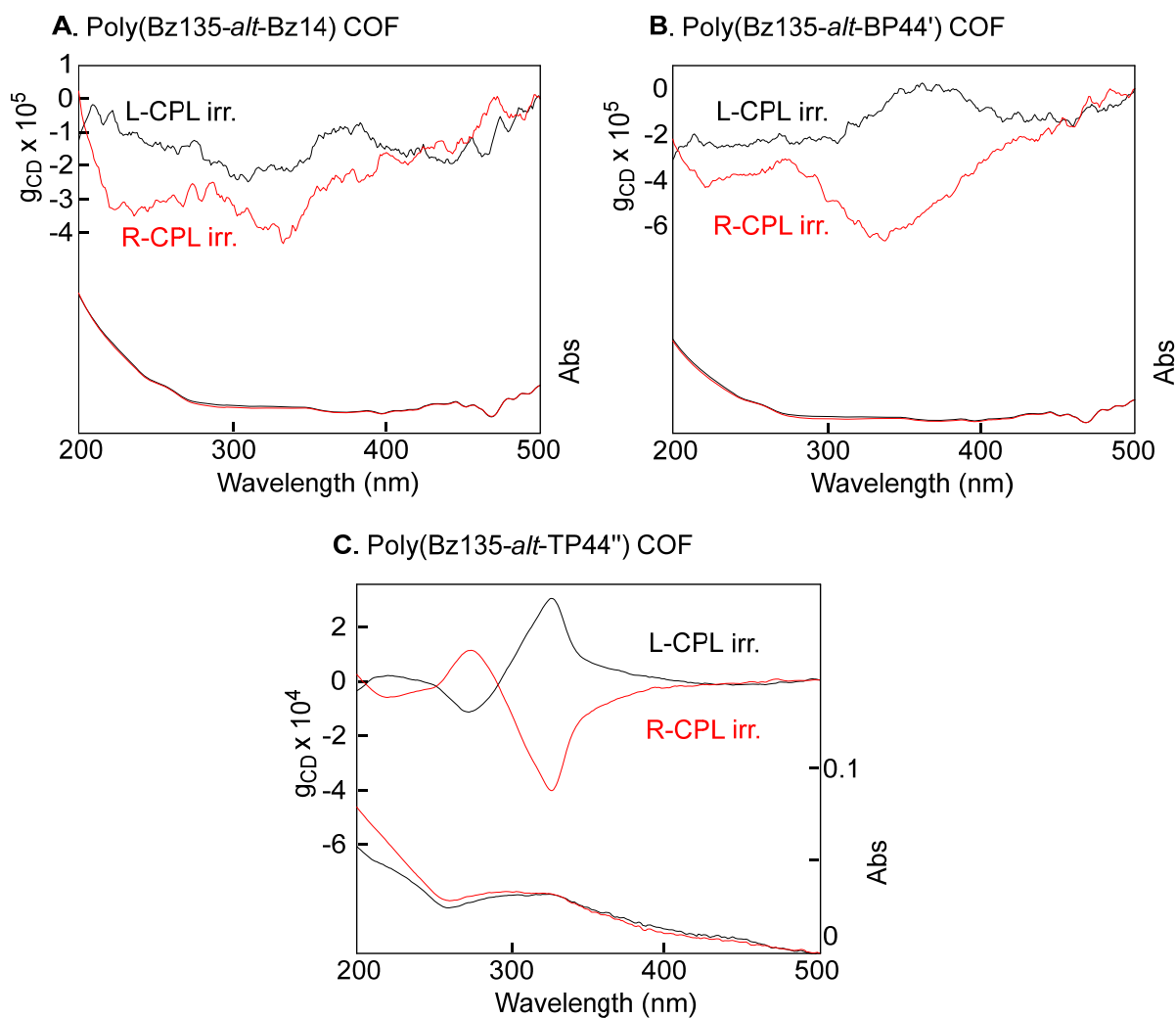


Fig. S17. g_{CD}-UV spectra of THF-insoluble COF's on L- and R-CPL irradiation: poly(Bz135-*alt*-Bz14) COF (run 4 in Table S1) (A), poly(Bz135-*alt*-BP44') COF (run 3 in Table S2) (B), and poly(Bz135-*alt*-TP44'') COF (run 3 in Table S3-1) (C). UV spectra in A and B were derived from HT spectra measured using the CD spectrometer. [Irradiation time = 20 min (A), 40 min (B), and 45 min (C)]

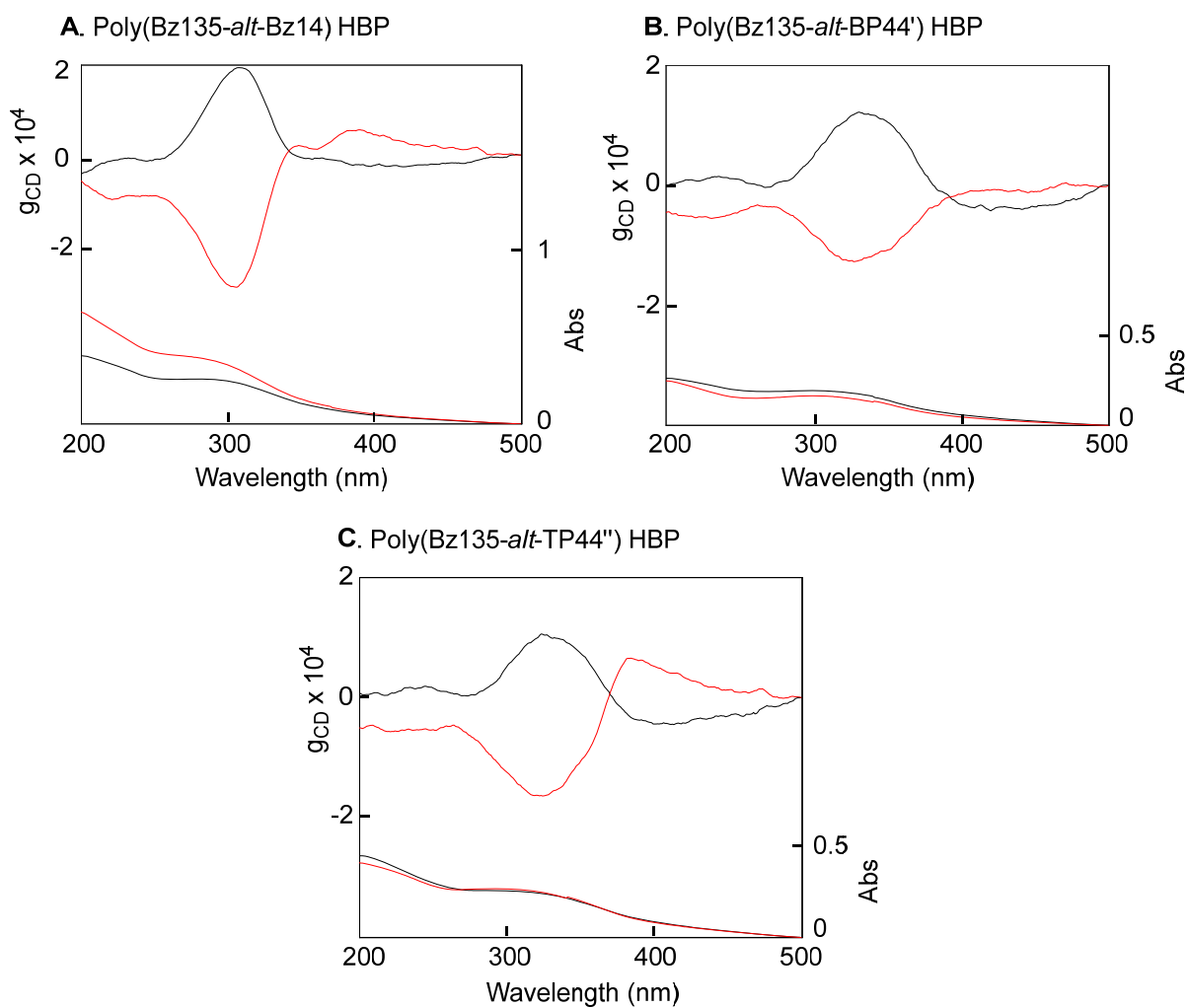


Fig. S18. g_{CD} -UV spectra of THF-soluble HBP's on L- and R-CPL irradiation: poly(Bz135-*alt*-Bz14) HPB (run 4 in Table S1) (A), poly(Bz135-*alt*-BP44') HBP (run 3 in Table S2) (B), and poly(Bz135-*alt*-TP44'') HBP (run 3 in Table S3-1) (C). [Irradiation time = 150 sec (A), 420 sec (B), and 600 sec (C)]

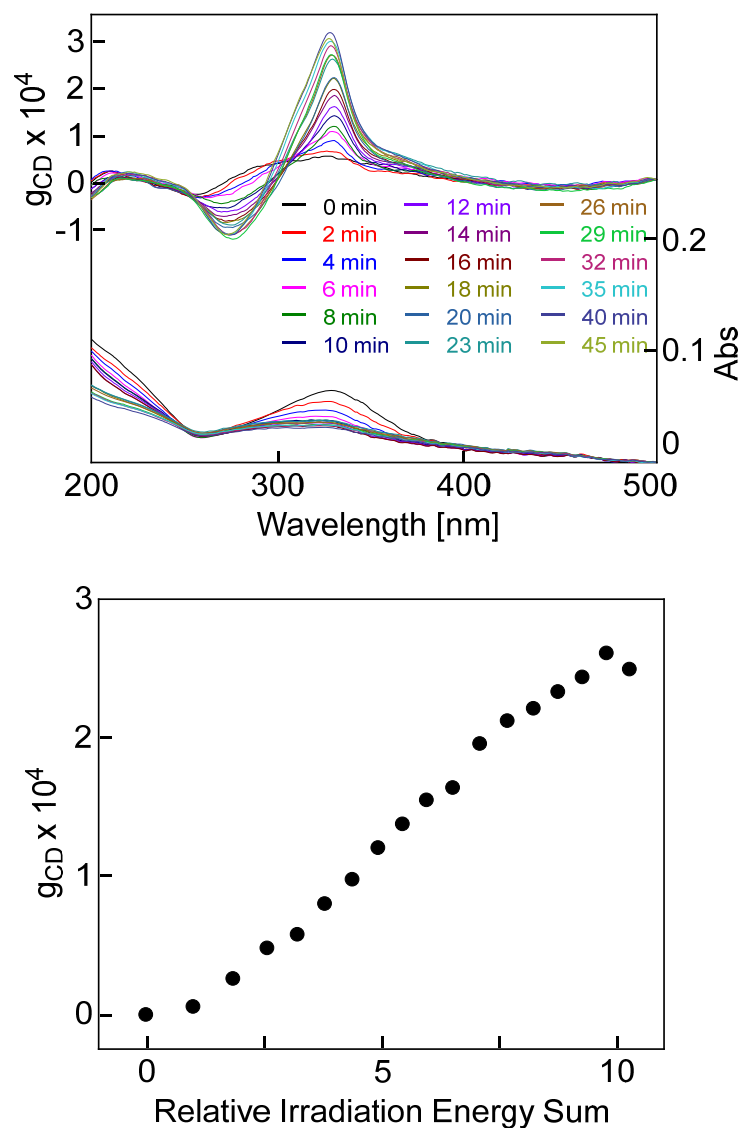


Fig. S19. g_{CD}-UV spectra observed after different durations of irradiation (top) and g_{CD}-vs.-relative irradiation energy sum plot (bottom) for THF-insoluble poly(Bz135-*alt*-TP44'') COF (run 3 in Table S3-1) in film corresponding to L-CPL irradiation.

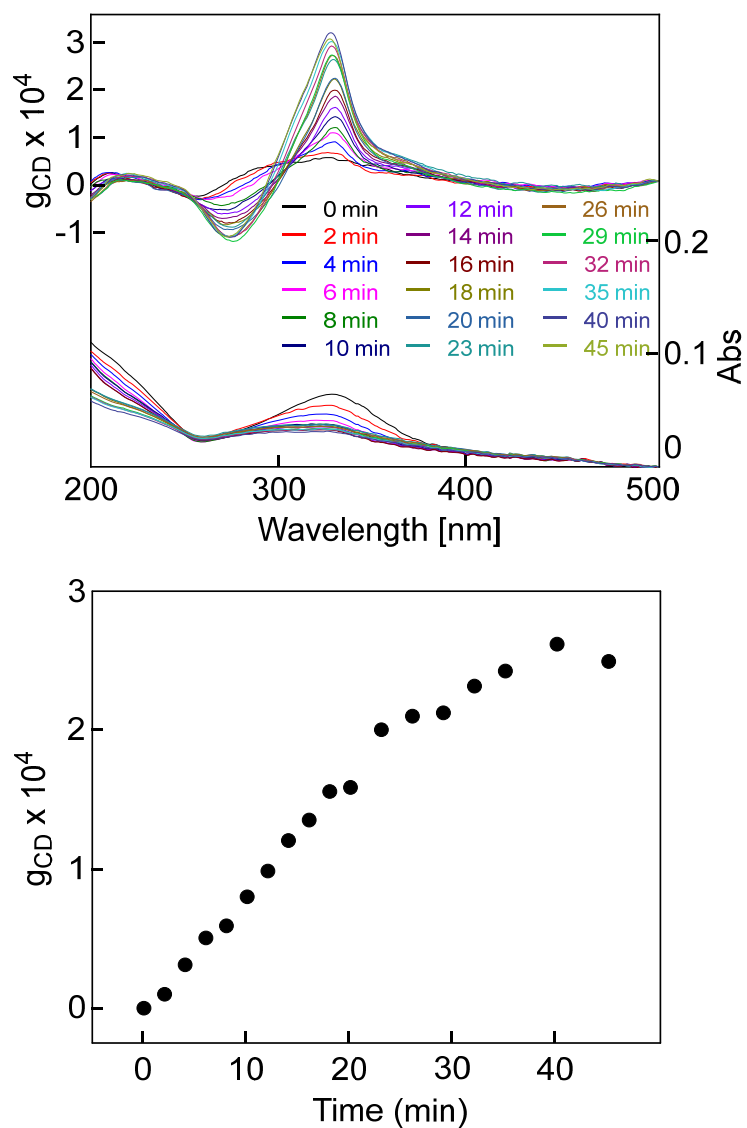


Fig. S20. g_{CD} -UV spectra observed after different durations of irradiation (top) and g_{CD} -vs.-irradiation time plot (bottom) for THF-insoluble poly(Bz135-*alt*-TP44'') COF (run 3 in Table S3-1) in film corresponding to L-CPL irradiation.

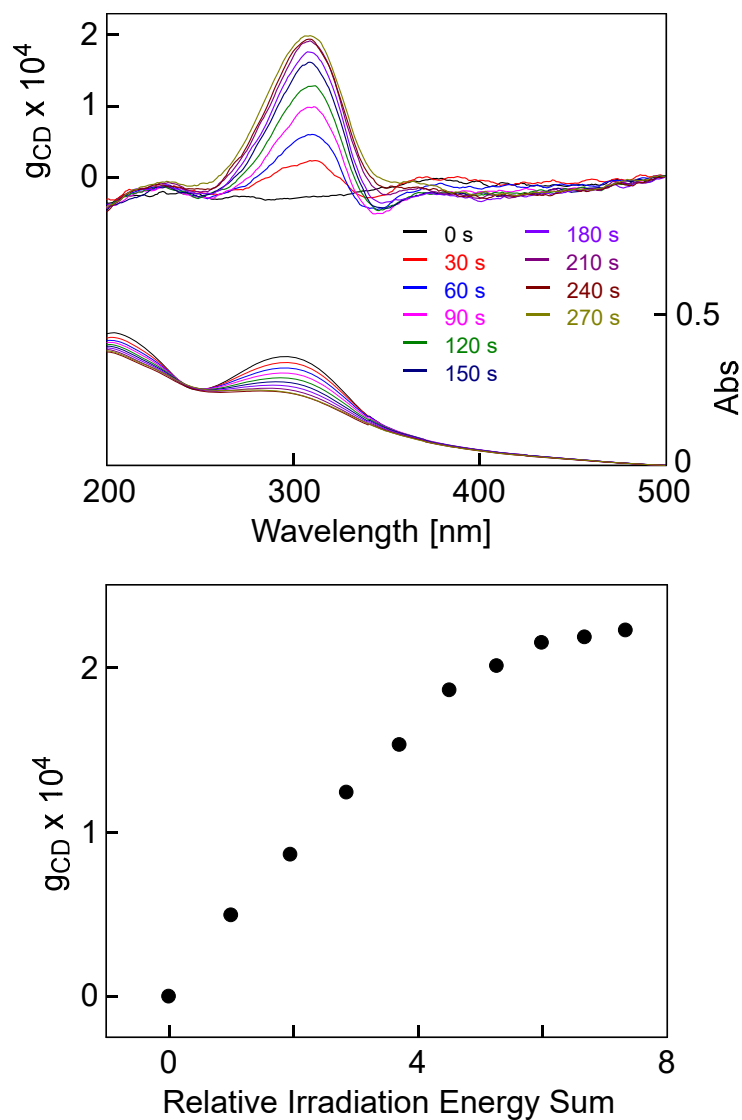


Fig. S21. g_{CD}-UV spectra observed after different durations of irradiation (top) and g_{CD}-vs.-relative irradiation energy sum plot (bottom) for THF-soluble poly(Bz135-*alt*-Bz14) HBP (run 4 in Table S1) in film corresponding to L-CPL irradiation.

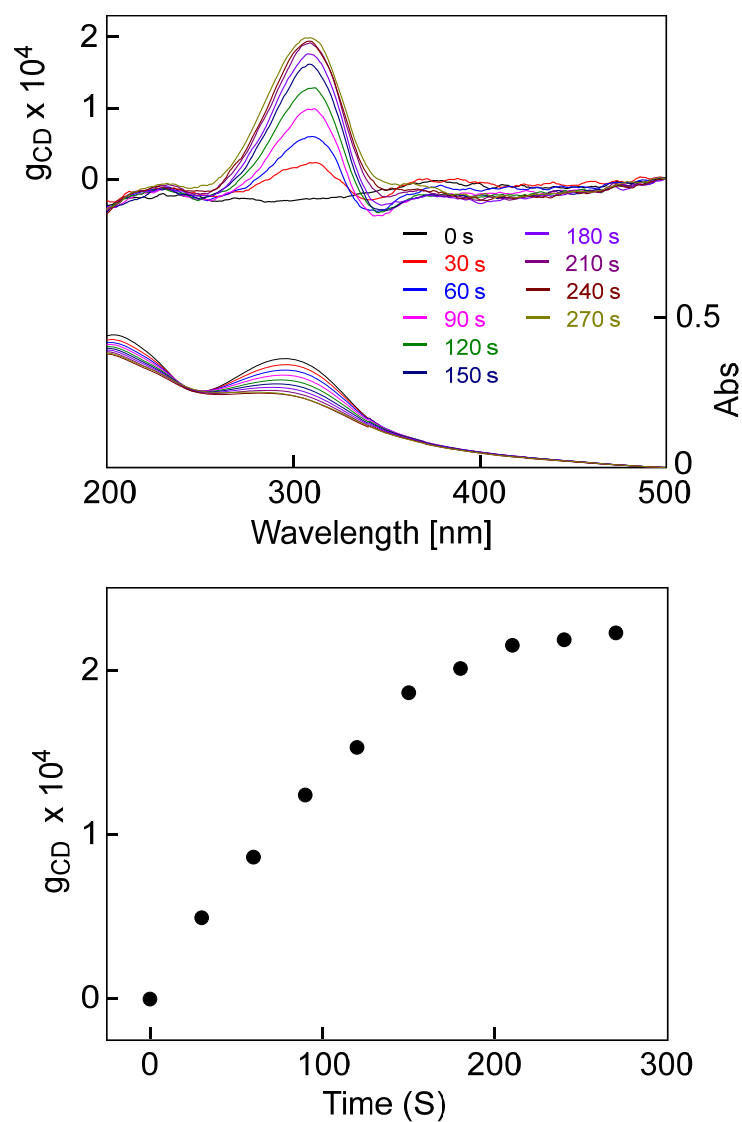


Fig. S22. g_{CD}-UV spectra observed after different durations of irradiation (top) and g_{CD}-vs.-irradiation time plot (bottom) for THF-soluble poly(Bz135-*alt*-Bz14) HBP (run 4 in Table S1) in film corresponding to L-CPL irradiation.

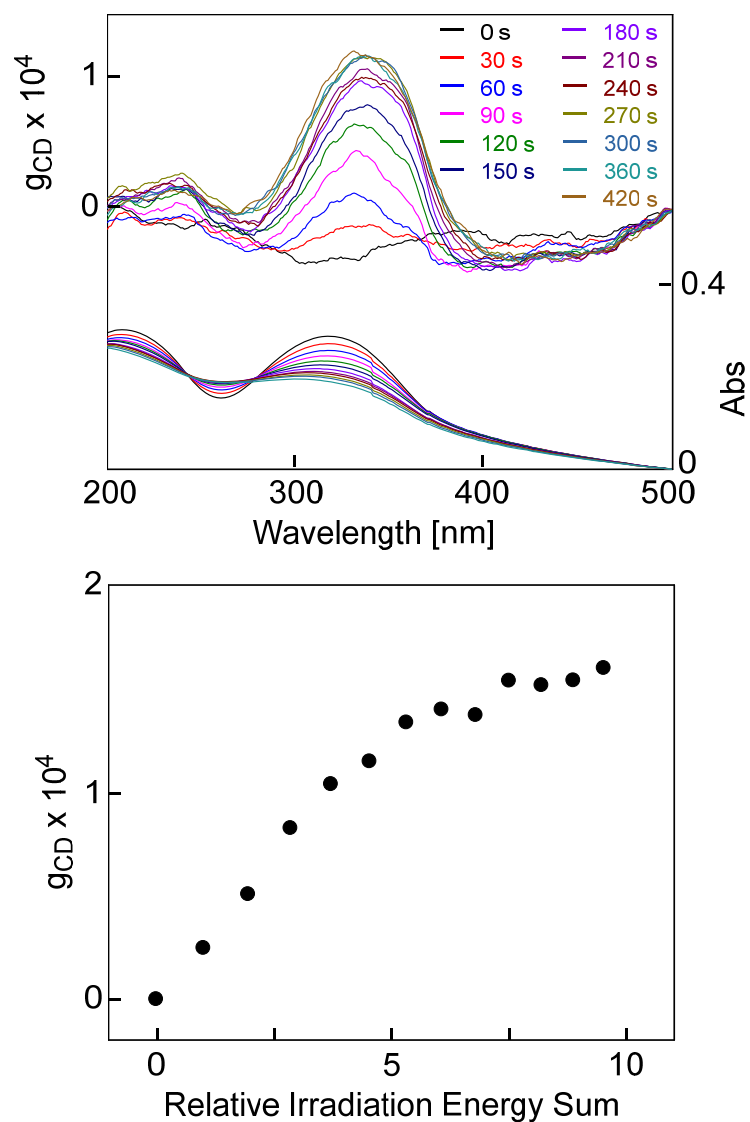


Fig. S23. g_{CD}-UV spectra observed after different durations of irradiation (top) and g_{CD}-vs.-relative irradiation energy sum plot (bottom) for THF-soluble poly(Bz135-*alt*-BP44') HBP (run 3 in Table S2) in film corresponding to L-CPL irradiation.

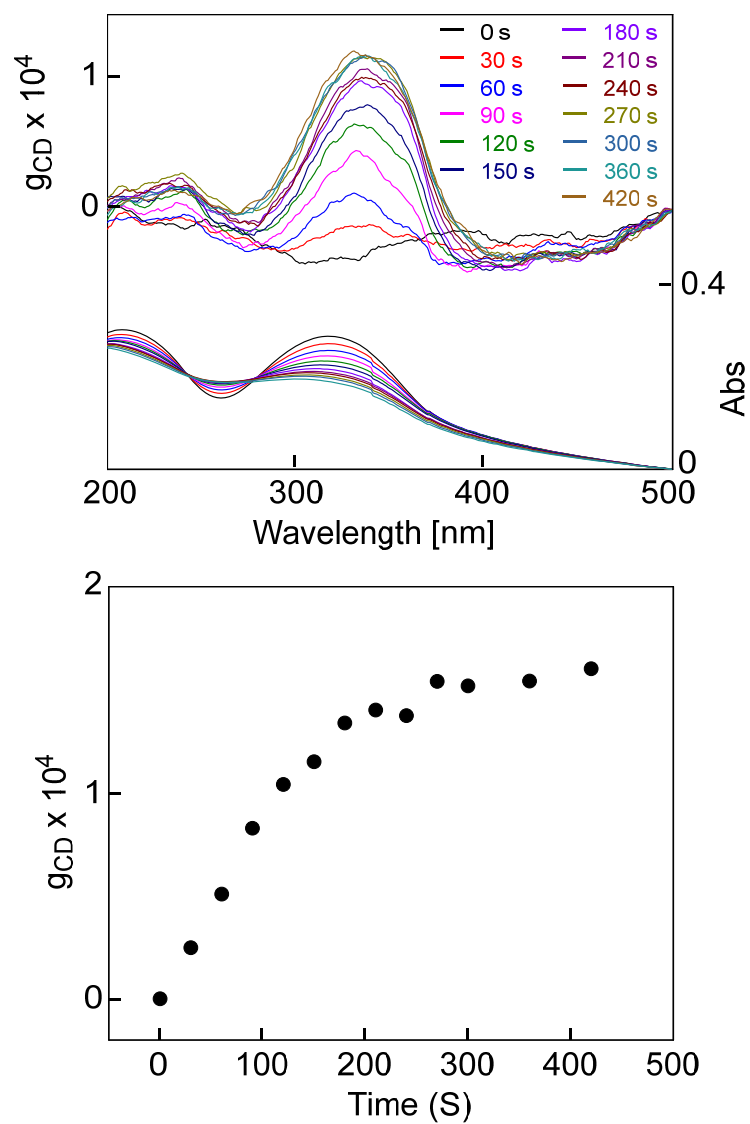


Fig. S24. g_{CD}-UV spectra observed after different durations of irradiation (top) and g_{CD}-vs.-irradiation time plot (bottom) for THF-soluble poly(Bz135-*alt*-BP44') HBP (run 3 in Table S2) in film corresponding to L-CPL irradiation.

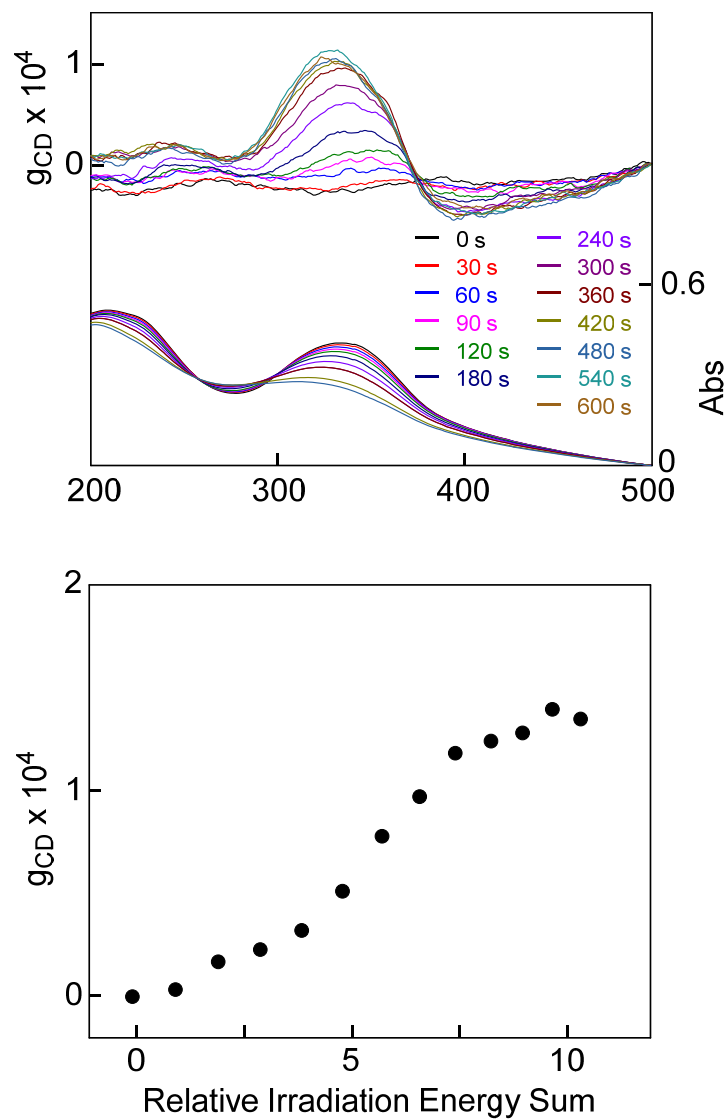


Fig. S25. g_{CD} -UV spectra observed after different durations of irradiation (top) and g_{CD} -vs.-relative irradiation energy sum plot (bottom) for THF-soluble poly(Bz135-*alt*-TP44'') HBP (run 3 in Table S3-1) in film corresponding to L-CPL irradiation.

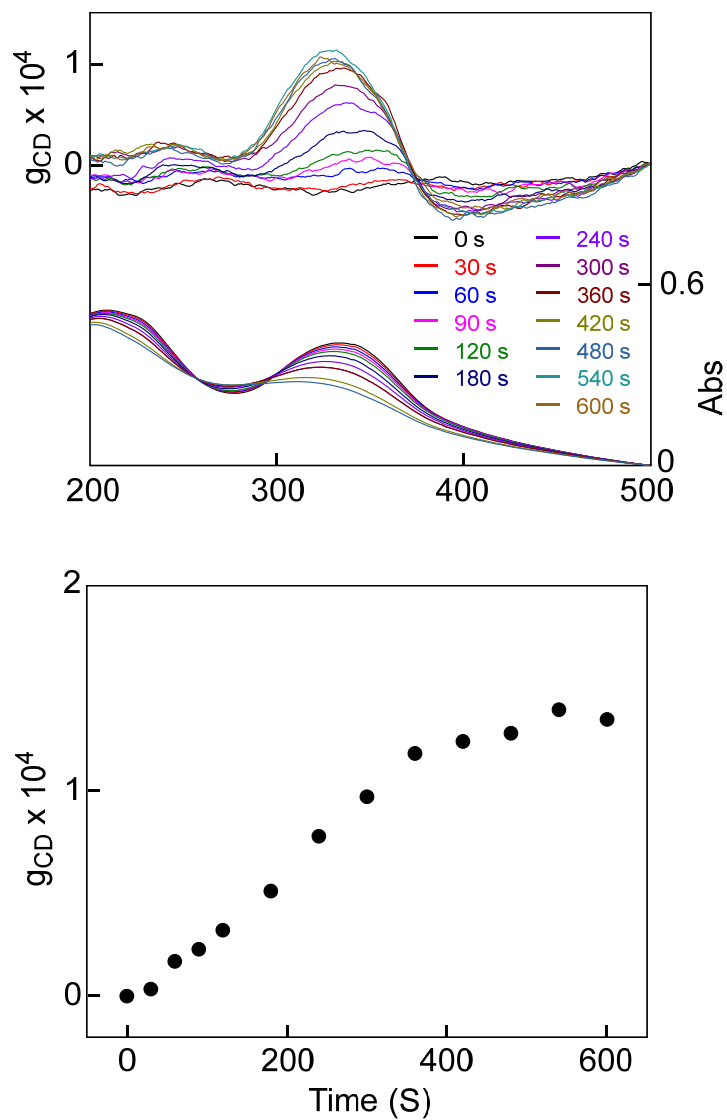


Fig. S26. g_{CD} -UV spectra observed after different durations of irradiation (top) and g_{CD} -vs.-irradiation time plot (bottom) for poly(Bz135-*alt*-TP44'') HBP (run 3 in Table S3-1) in film (run 3 in Table S2) corresponding to L-CPL irradiation.

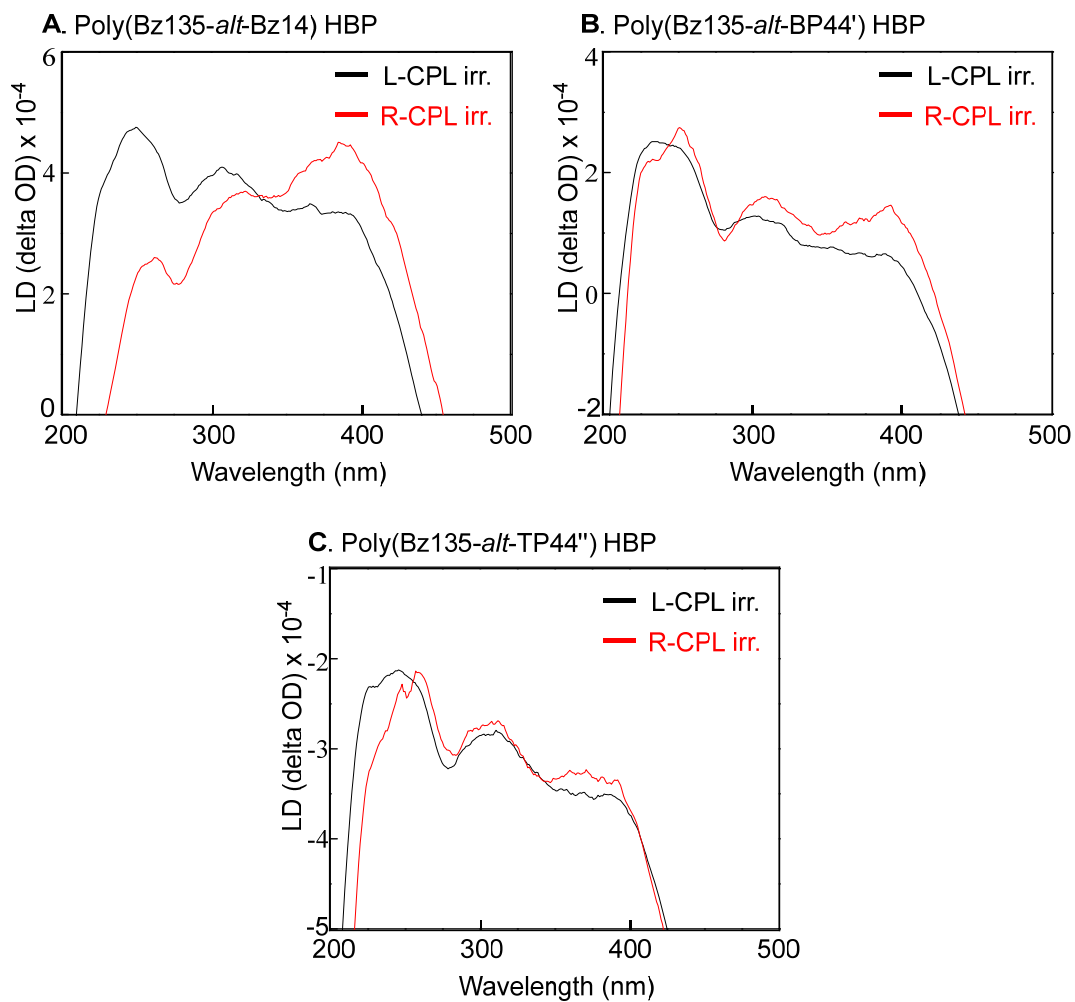


Fig. S27. Linear dichroism (LD) spectra of THF-soluble poly(Bz135-*alt*-Bz14) HBP (run 4 in Table S1) (A), poly(Bz135-*alt*-BP44') HBP (run 3 in Table S2) (B), and poly(Bz135-*alt*-TP44'') HBP (run 3 Table S3-2) (C) in film observed on CPL irradiation.

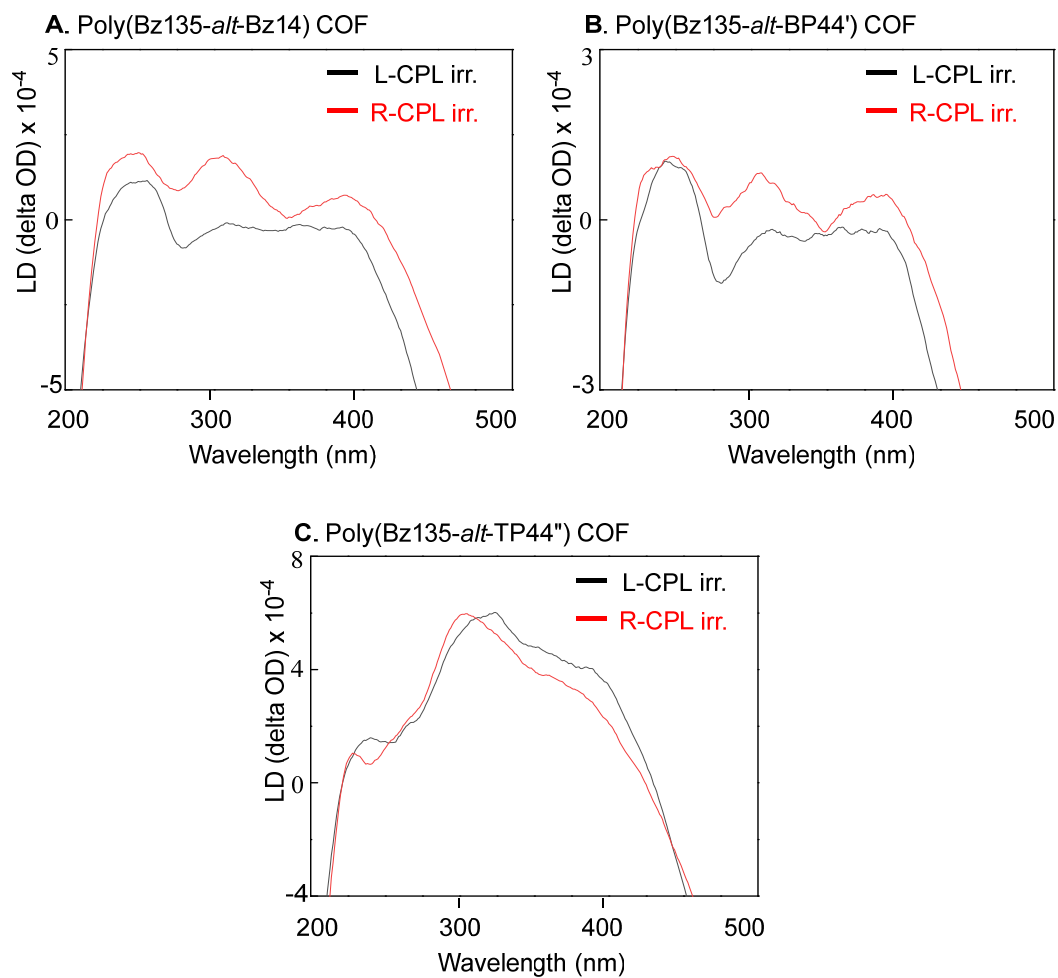


Fig. S28. Linear dichroism (LD) spectra of THF-insoluble poly(Bz135-*alt*-Bz14) COF (run 4 in Table S1) (A), poly(Bz135-*alt*-BP44') COF (run 3 in Table S2) (B), and poly(Bz135-*alt*-TP44'') COF (run 3 Table S3-2) (C) in film observed on CPL irradiation.

Table S4. BET analysis of THF-insoluble poly(Bz135-*alt*-Bz14) COF's (**Table S1**), poly(Bz135-*alt*-BP44') COF's (**Table S2**) and poly(Bz135-*alt*-TP44'') COF's (**Table S3-1**)

COF	[L]/[C] in feed	Surface area (m ² /g)	Total pore volume (cc/g)
Poly(Bz135- <i>alt</i> -Bz14)	2/1	4.6	0.0109
	3/1	26.9	0.0423
	4/1	11.0	0.0378
Poly(Bz135- <i>alt</i> -BP44')	2/1	64.3	0.0532
	3/1	31.6	0.0547
	4/1	22.4	0.0526
Poly(Bz135- <i>alt</i> -TP44'')	1/1	15.7	0.0272
	1.5/1	29.0	0.0334
	2/1	11.6	0.0200
	2/1 ^a	18.5	0.0532
	3/1	29.8	0.0434
	4/1	16.5	0.0316

^arun 3 in Table S3-2.

References

1. R. K. Harris, E. D. Becker, S. M. Cabral De Menezes, P. Granger, R. E. Hoffman, K. W. Zilm, Further conventions for NMR shielding and chemical shifts IUPAC recommendations 2008. *Solid State Nuclear Magnetic Resonance* **2008**, *33* (3), 41-56.
2. A. E. Bennett, C. M. Rienstra, M. Auger, K. Lakshmi, R. G. Griffin, Heteronuclear decoupling in rotating solids, *J. Chem. Phys.* **1995**, *103* (16), 6951-6958.
3. E. DeAzevedo, R. Franco, A. Marletta, R. Faria, T. Bonagamba, Conformational dynamics of phenylene rings in poly (p-phenylene vinylene) as revealed by ¹³C magic-angle-spinning exchange nuclear magnetic resonance experiments. *J. Chem. Phys.* **2003**, *119* (5), 2923-2934.
4. S. M. Jansze, D. Ortiz, F. Fadaei Tirani, R. Scopelliti, L. Menin, K. Severin, Inflating face-capped Pd₆L₈ coordination cages, *Chem. Commun.* **2018**, *54* (68), 9529-9532.